

## Investigation of Spatial Characteristics of Multi-Phase AC Arc Combined with In-Situ Particle Measurement

Y. Liu<sup>1</sup>, M. Tanaka<sup>1</sup>, S. Choi<sup>1</sup> and T. Watanabe<sup>1,2</sup>

<sup>1</sup>Dept. Environmental of Chemistry and Engineering, Tokyo Institute of Technology, Yokohama, Japan

<sup>2</sup>Dept. Chemical Engineering, Kyushu University, Fukuoka, Japan

**Abstract:** A multi-phase alternating current (AC) arc has been developed for time and energy saving in glass production. The spatial characteristics of the arc discharge were examined and in-situ particle measurements were conducted to investigate effects of plasma temperature distribution on the in-flight particles. Result shows the difference in temperature at various radial positions was caused by the spatial nonuniformity of arc and electrode configurations.

**Keywords:** Multi-phase AC arc, in-flight melting, high-speed camera, two-color pyrometry

### 1. Introduction

The Siemens-type melter has been used over 140 years in glass industry because of its superior large-scale performance and continuous melting system. Glass production requires considerable energy to sustain the very high temperature needed to melt the glass batch. Lots of byproducts like CO<sub>2</sub>, NO<sub>x</sub>, etc. are produced due to the usage of fossil fuel, which brings about environmental pollution.

Thermal plasma has been introduced in industrial glass-making during the second half of the 20th century. Among various thermal plasma reactors, multi-phase AC arc process has the following advantages: high energy efficiency, large volume, low velocity, easy scale up, and low cost [1-3]. Up to date, very few studies have been undertaken to analyze the influence of multi-phase arc on the characteristics of in-flight glass particles [4]. The correlation between the temporal arc fluctuation and the in-flight particle temperature has been approved in our previous work [5]. The objective in this work is to understand the spatial characteristics of multi-phase arc by high-speed video observation combined with in-situ particle measurement. The electrode configuration, carrier gas flow and radial position in the plasma region are known to significantly influence the plasma properties so as to affect the in-flight particle characteristics.

### 2. Experimental

#### 2.1 System description

**Figure 1** gives a schematic diagram of the experimental setup for the arc discharge behavior measurement in the 12-phase AC arc plasma system. The 12 electrodes made of 2%-thoriated tungsten with a diameter of 6 mm. They were divided into two layers to produce the plasma. The angle between the upper six inclined electrodes and the six lower horizontal electrodes was 30°. A servomotor system is used to precisely control the electrode position. Argon gas with purity of 99.99% was injected around

each electrode at a flow rate of 5 L/min to prevent it from oxidation.

#### 2.2 Arc discharge behavior measurement system

**Figure 2** illustrates two kinds of electrode configurations for generating the 12-phase arc. The discharge behaviors of arc were characterized by a

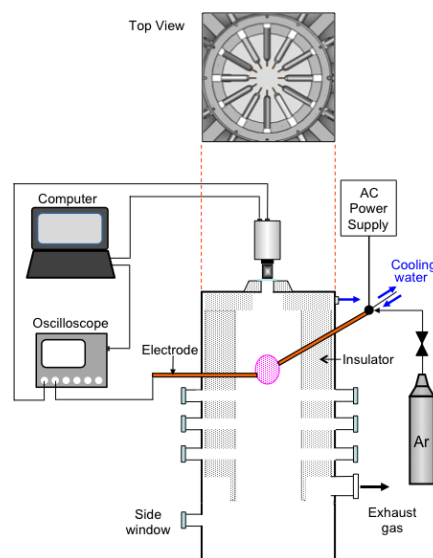


Fig. 1 Schematic of the multi-phase AC arc apparatus with arc discharge behavior measurement system.

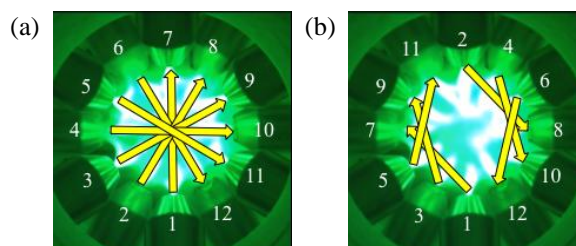


Fig. 2 Electrode configurations of 12-phase AC arc: (a) Clockwise pattern and (b) Flip-flop pattern.

high-speed video camera. After the ignition, the upper six electrodes were mounted a circle of 80 mm, while the lower six were backed off at a distance of 100 mm. The camera was installed on the top of the arc chamber and the top view of the multi-phase AC arc was recorded. The camera recorded at a speed of 10000 frames/s with a shutter speed of 0.37  $\mu$ s.

### 2.3 Particle measurement systems

Raw materials of alkali-free glass raw materials with an average grain size of 135  $\mu$ m were prepared by the spray-drying method from the reagents of  $H_3BO_3$ ,  $Al_2O_3$ ,  $BaCO_3$ , and  $SiO_2$ .

The high-speed pyrometry system used for particle measurement is DPV-2000 (Tecnar, Canada). The sensing head was positioned at the constant height of 80 mm down from the electrodes and varied along the radial position. An optical two-slits photomask is inserted at the end of the center fiber inside the sensing head. When a hot particle crosses the sensor measurement volume, an image with two peaks is recorded through the photomask [6]. The thermal radiance emitted by a particle is filtered by two wavelength bands,  $\lambda_1=787 \pm 25$  nm and  $\lambda_2=995 \pm 25$  nm, respectively. According to our previous research [4], the particle temperature obtained by DPV-2000 is not the real surface temperature. To quantify the influence of non-thermal radiations on the total radiations by collected DPV-2000, calibration method was investigated by a spectrometer (MicroHR, Horiba).

## 3. Experimental Results

### 3.1 High speed imaging analysis of the plasma

The captured videos were saved to individual images at the interval of 0.1 ms. Each image was then transformed into binary images with black and white by setting an appropriate threshold value. The luminance area is assumed to be the arc existence area or the high temperature area. **Figure 3** shows the arc existence areas generated by different electrode configurations and accumulated in 10 ms. The distribution was obtained by averaged luminance value calculated over 10 discharge cycles in consideration of the variability of the process. The arc in clockwise (CW) pattern is distributed more uniformly, while the high temperature region was concentrated around the electrode and relatively low in the flip-flop (FF) pattern.

One of the most important characteristics of the multi-phase arc is the periodical swinging motion of the arc spot [7]. **Figure 4** gives the contour maps of the existence time of the arc at the electrode region. Larger arc swing angle caused wider distributed high temperature region. Uniform temperature distribution is expected for homogeneous powder treatment.

The effect of different diameter of tungsten electrode on

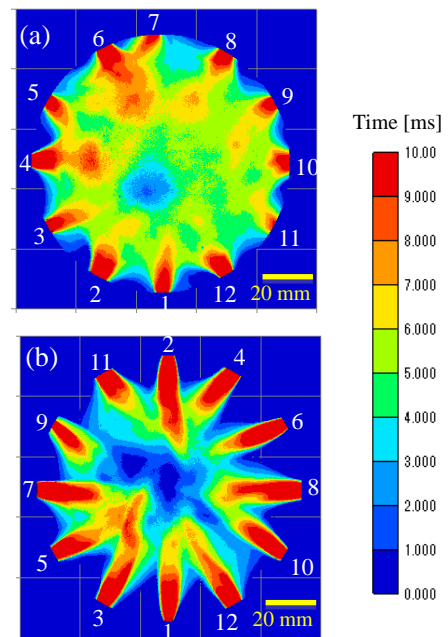


Fig. 3 Arc existence time of the 12-phase AC arc during an AC cycle: (a) CW pattern and (b) FF pattern.

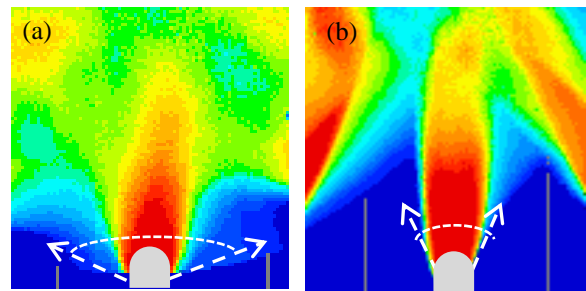


Fig. 4 Contour map of the existence time of 12-phase AC arc with different electrode configurations: (a) CW pattern and (b) FF pattern.

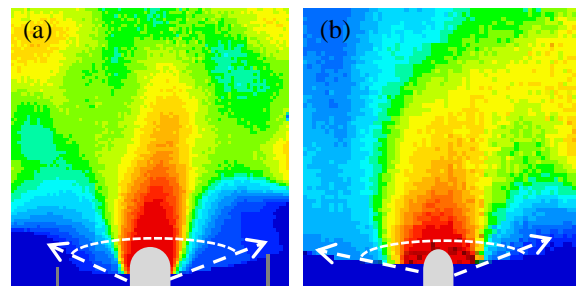


Fig. 5 Contour map of the existence time of 12-phase AC arc with different tungsten diameter: (a) 6 mm and (b) 3.2 mm.



the arc swinging angle was also investigated. The contour maps in **Fig. 5** show that the smaller electrode diameter results in wider arc swing. The control of the arc existence area must play an important role in powder treatment using the multi-phase AC arc plasma.

### 3.2 Spatial characteristics of in-flight particles

Experiments were considered under three parameters including electrode configuration, radial position and carrier gas flow rate. Powder feed rate was fixed at 30 g/min and carrier gas flow rate was varied at 10, 20 and 30 L/min. Five different radial distances were measured from the center of the plasma flame. Signals of individual particles called “good particles” were collected until a satisfactory number was obtained, usually more than two thousands.

The effect of carrier gas flow rate on the average axial velocity of particles at different radial positions in CW and FF patterns are shown in **Fig. 6**. At each constant flow rate, particles have the maximum velocity in the center of plasma region and decrease along the radial position. Particle velocity increased with increasing the

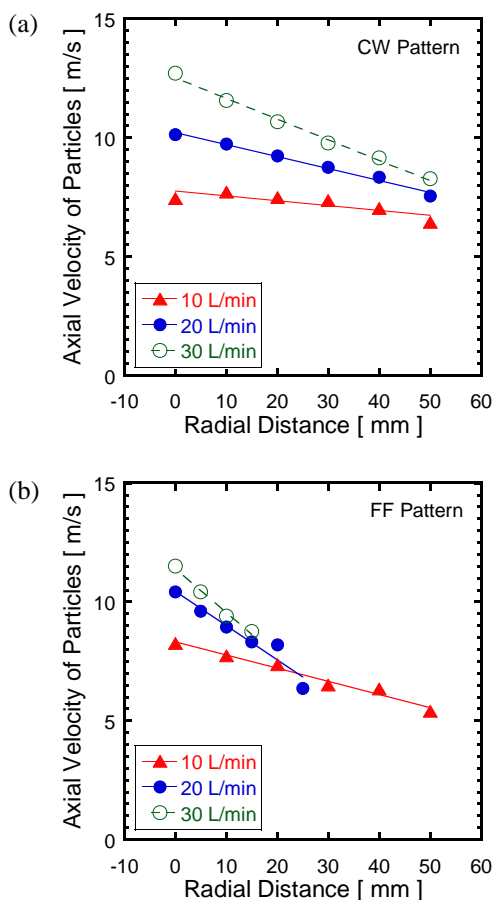


Fig. 6 Variation of average axial velocity at different radial distance: (a) CW pattern and (b) FF pattern.

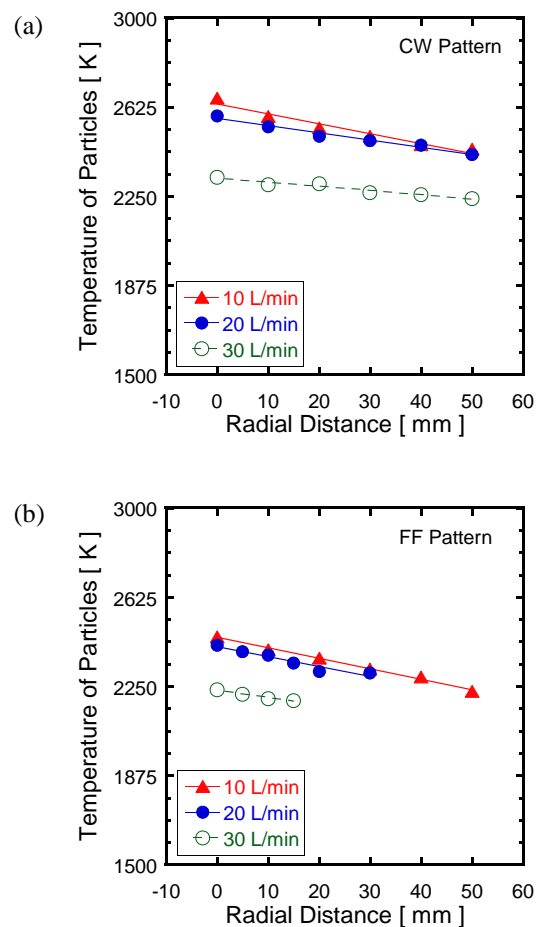


Fig. 7 Variation of average temperature at different radial distance: (a) CW pattern and (b) FF pattern.

carrier gas flow rate, and the dispersion in particle velocity becomes larger. Moreover, the axial velocity of particles in FF pattern is little higher than that of CW pattern in the central area. It should be noted that there was small number of particles can be detected further away from the plasma center line in FF pattern, especially at higher carrier gas flow rate. The particle detection rate in FF pattern was higher than that of CW pattern in the central area. From the arc existence area shown in Fig. 3, it can be considered that the arc region has high temperature and viscosity. The arc path was mainly closed to the electrodes in FF pattern, and therefore, the particles can pass through the center of plasma region more easily.

**Figure 7** shows variation of average temperature according to the radial distance for various carrier gas flow rate in CW and FF patterns. From both of the figures, average particle temperature varies linearly with the radial distance. Moreover, particles have the maximum temperature in the center of plasma region and decrease along the radial position. The temperature difference between carrier gas flow rates of 10 and 20 L/min are not obvious, however, the temperature decrease rapidly at 30

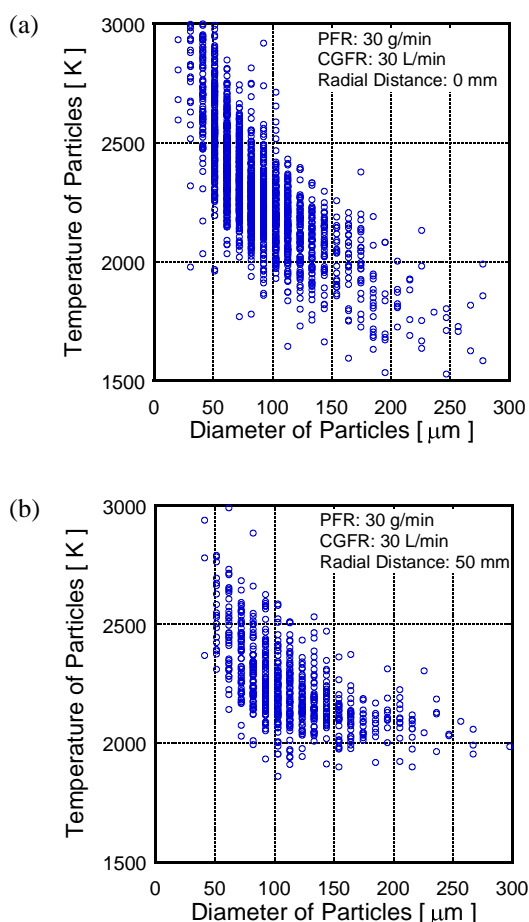


Fig. 8 Relationship of particle diameter and temperature estimated by DPV-2000 at different radial distance in CW pattern: (a) radial distance at 0 mm and (b) radial distance at 50 mm.

L/min. This indicates that the particles at lower carrier gas flow conditions are well melted.

**Figure 8** presents the overall distributions of particle diameter versus their temperatures obtained by DPV-2000 at different radial distance in CW pattern. The particles are tended to have smaller diameter in the center line of plasma. As was discussed before, the particle temperature decreased with increasing of radial distance. Therefore, the particles can be well melted near the center line of the plasma, thus their particle size decreased.

Other experimental results showed that during the powder injection, larger raw particles are preferably localized on the center line before their entry into the plasma. Increase of carrier gas flow rate results in a narrow spread of particles in plasma flame. Thus an increase of smaller particles can be found at the center region of plasma.

#### 4. Conclusion

The spatial characteristics of multi-phase AC arc with different electrode configurations have been investigated for the first time. The arc swinging angle was contributed to the high temperature distribution of the multi-phase arc. The spatial characteristics of particle temperature and axial velocity were investigated by DPV-2000 and spectroscopic measurement. Experimental studies have identified that the spatial characteristics of particles are related with different electrode configurations. The probability of detected particles was low far away from the central area due to high viscosity near the electrode region in FF pattern. The spatial characteristics of in-flight particles are demonstrated to be affected by electrode configuration, radial position and carrier gas flow rate. This study provides important information to understand the plasma-particle energy exchange dynamics. Efficient in-flight glass melting can be achieved by adjusting electrode configuration.

#### 5. Acknowledgments

The financial support provided by the Strategic Development of Energy Conservation Technology Project of NEDO (New Energy and Industry Technology Development Organization, Japan) is gratefully acknowledged.

#### 6. References

- [1] Y. Yao, K. Yatsuda, T. Watanabe and T. Yano, *Plasma Science and Technology*, **11**, 699 (2009).
- [2] Y. Yao, K. Yatsuda, T. Watanabe, T. Matsuura and T. Yano, *Plasma Chemistry and Plasma Processing*, **29**, 333 (2009).
- [3] T. Watanabe, K. Yatsuda, Y. Yao, T. Yano and T. Matsuura, *Pure and Applied Chemistry*, **82**, 1337 (2009).
- [4] Y. Liu, M. Tanaka, S. Choi and T. Watanabe, *Journal of Thermal Spray Technology*, **21**, 863 (2011)
- [5] Y. Liu, M. Tanaka, T. Ikeba, S. Choi and T. Watanabe, *Abstracts of the 12th High-Tech Plasma Processing*, **136** (2012).
- [6] M. Krauss, D. Bergmann, U. Fritsching and K. Bauckhage, *Material Science and Engineering*, **326**, 154 (2002).
- [7] M. Tanaka, Y. Tsuruoka, Y. Liu, T. Matsuura and T. Watanabe, *IEEE Transactions on Plasma Science*, **39**, 2904 (2011).